Int. J. Electrochem. Sci., 9 **(2014)** 22 – 31

International Journal of
ELECTROCHEMICAL
SCIENCE
www.electrochemsci.org

Polyacrylonitril Electrospun Nanofiber As a Template to Prepare NiO Nanostructure Electrocatalyst

Ahmed Elzatahry[1,2]

[1]Department of chemistry, King Saud University, PO Box: 2455, Riyadh 11451, Riyadh, Kingdom of Saudi Arabia.
[2]Advanced Technology and New Materials Research Institute, City of Scientific Research and Technology Applications, New Borg El Arab City, Alexandria, Egypt.
[*]E-mail: aelzatahry@ksu.edu.sa

Received: 26 June 2013 / *Accepted:* 2 September 2013 / *Published:* 15 November 2013

The present work explores a facile route to synthesize NiO nanofibers using a hybrid method based on a combination of electrospinning and calcination techniques. Poly acrylonitrile was used as a template matrix to maintain the nanostructrure of produced NiO. The as-prepared nanostructured material was characterized with X-ray diffraction (XRD), energy dispersive X-Ray (EDX), and scanning electron microscopy (SEM), respectively. The electrochemical properties towards methanol oxidation have been studied using cyclic voltametry and Cchronoamperometry technique. Electrocatalytic oxidation of methanol on prepared NiO nanostructure in a potential range of 0–800 mV (versus SCE) is studied by cyclic voltammetry in alkaline medium (1.0 M KOH). Prepared NiO nanostructure showed an interesting activity towards methanol oxidation. The effect of scan rate has been studied and the process has approved to be diffuse rather than surface controlled.

Keywords: Nanofibers, Nickel Oxide, Electrospinning, Methanol oxidation, Electrocatalyst.

1. INTRODUCTION

Electrospinning is an efficient and outstanding technique to fabricate polymer nanofibers [1]. Many polymers have been successfully electrospun into fibers such as Polyacrylonitrile, PAN [2], Polyvinyl alcohol, PVA [3], PVC [4] Polyethylene oxide, PEO [5],….etc [1]. Polymer nanofibers produced by electrospinning technique have several interesting features such as “high surface area, high porosity, good mechanical properties, high and cost effectiveness” [6]. Different composite with various compositions have also produced using electrospining technique [6-9] For different applications such as sensors [8, 10], biomedicals [11-13], energy [14] and many technological applications [15].

Nickel oxide (NiO) has been used in several fields, such as dye-sensitized solar [16], gas sensor [17], fuel cell [18] and catalysis [19]. On the other hand, several techniques have been used to prepare NiO nanostructures, including hydrothermal growth method [20], sol-gel method [20, 21], electro deposition [22], sputtering [23] and chemical vapor deposition [24]. Recently, electrospinning technique is used to prepare Porous NiO fibers for Li-ion batteries application [25]. In this study, we describe the synthesis of nanostructure NiO electrocatalyst based on elctrospun fibers template. The fiber template is prepared by electrospinning a solution mixture of polyacrylonitrile and 50 wt % NiO. The results indicate that prepared NiO electrocatalysts has an interesting activity in electrochemical oxidation of methanol in alkaline medium.

2. EXPERIMENTAL

2.1 Carbon naofibers preparation

10 g of PAN (150,000 g/mol) was dissolved in Dimethyl formamide (DMF) at 25 ^{o}C under continuous stirring for 3 h., then 5 g of Nickel(II) nitrate hexahydrate was added and the resultant solution was stirred at 25°C for 3 h.

Electrospun fibers were produced by electrospinning prepared solution at a potential of 20 kV using A 10 ml syringe with a metal needle , which kept at a distance of 17 cm from aluminum collecting drum covered with an aluminum foil. The flow rate was adjusted to be 0.5 ml/hour using a syringe pump (Schematic diagram 1). Prepared electrospun fibers were collected and dried at 50 °C under vacuum. Nanostructure NiO nanofibers were prepared during heat treatment step (Calcination process) at 400 $^{\circ}$C in the air for 3.5 h.

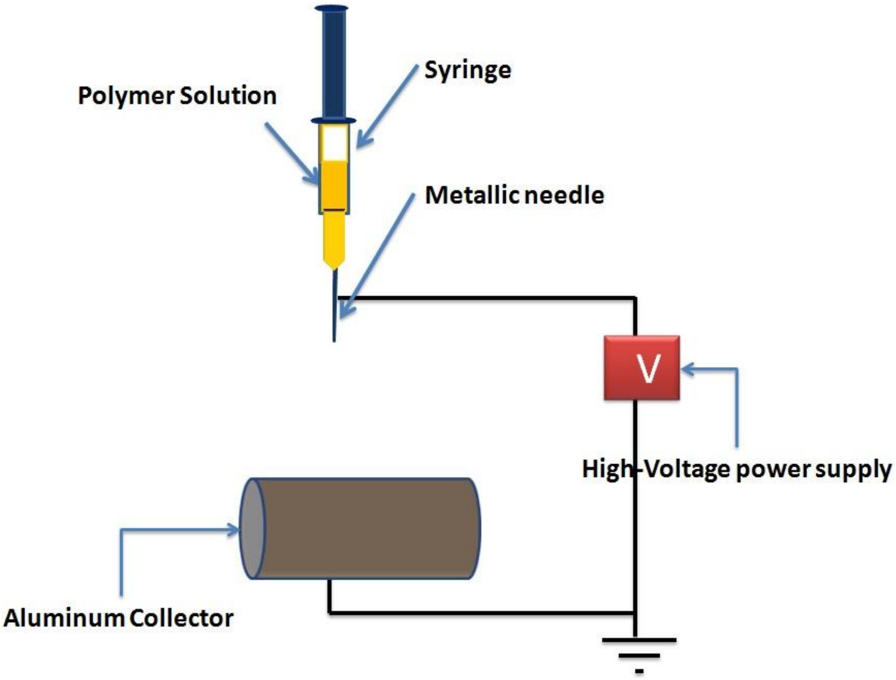

Schematic Diagram 1: Typical electrospinning setup of the electrospinning process.

2.2. Materials characterization

X-ray diffracttometer using CuKα radiation (XRD, Bruker D8 Advance X-ray diffractometer), and thermal field emission scanning electron microscopy (JSM-7100F) were used to evaluate the crystal structure and The morphology- the composition of the as-prepared materials, respectively.

2.3. Electrochemical measurements

Electrochemical activities of prepared nanomaterials were measured using Gamry Interface 1000 Potentiostats/Galvanostats/ZRA [26]. The cyclic Voltammetry (CV) curves were collected with a potential window from 0. 0 to +0.8 V (vs. SCE) at a scan rate of 20 mV s−1 in 6M KOH and a potential window from 0. 0 to +0.8 V (vs. SCE) at different scan rates from 1 mV s−1 of 100 mV s−1 In 1.0 M MeOH/6 M KOH for methanol oxidation measurements. All the measurements have been done in Dr. Bob’s Pyrex glass cell against Saturated Calomel Reference Electrode (SCE). The counter electrode was a Pt wire or 1 mm diameter and 15 cm long. Working electrodes were fabricated as following:

First step, 0.1 mg of carbon Vulcan xc-72 in 0.5 ml isopropyl alcohol and placing it in an ultrasonic bath for 30 min, 10μL of the dispersion was deposited onto a glassy carbon (GC) disk electrode followed by one drop of Nafion solution (10 wt.%) and left to dry for 6 h. the second step was achieved by dispersion a 0.1 mg of the prepared NiO nanostructure materials in 0.5 ml isopropyl alcohol and placing it in an ultrasonic bath for 30 min, 30μL of the dispersion was deposited onto a carbon vulcan xc-72/glassy carbon (GC) disk electrode followed by one drop of Nafion solution (10 wt.%) and left to dry overnight.

3. RESULTS AND DISCUSSION

3.1 Physical Characterization

The morphology of the as-prepared PAN/ Nickel(II) nitrate hexahydrate electrospun fibers was observed by means of field emission scanning electron microscopy (FESEM) at different magnification, as presented in Figure 1a,b. The FESEM images reveal a sub-micron, random, uniform fibers, and the size distribution of the produced elctrospun fibers was almost uniform and the diameter of the electrospun fibers was 145–170 nm. Figure 2.a,b show the interesting morphology of electrospun fiber after calcinations at 400 ^{o}C for 3.5 h in air. The images present the porous structure formed after removal of PAN polymer template as a result of heat treatment. The results came in agreement with results reported by Wang et.al [25]. The elemental composition of NiO according to EDX analysis after calcination process is presented in Figure 3. The data reveal the presence of Ni and O with higher weight ratio compared to carbon after calcinations, which gives a strong indication for the removed of polymer template during the heat treatment process.

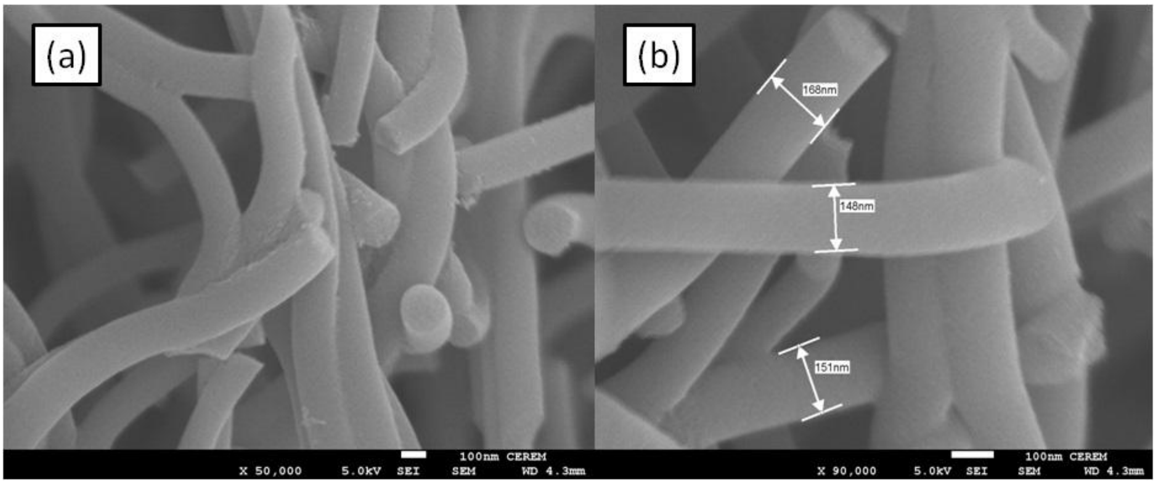

Figure 1. FESEM images of PAN/ Nickel(II) nitrate hexahydrate electrospun fibers.

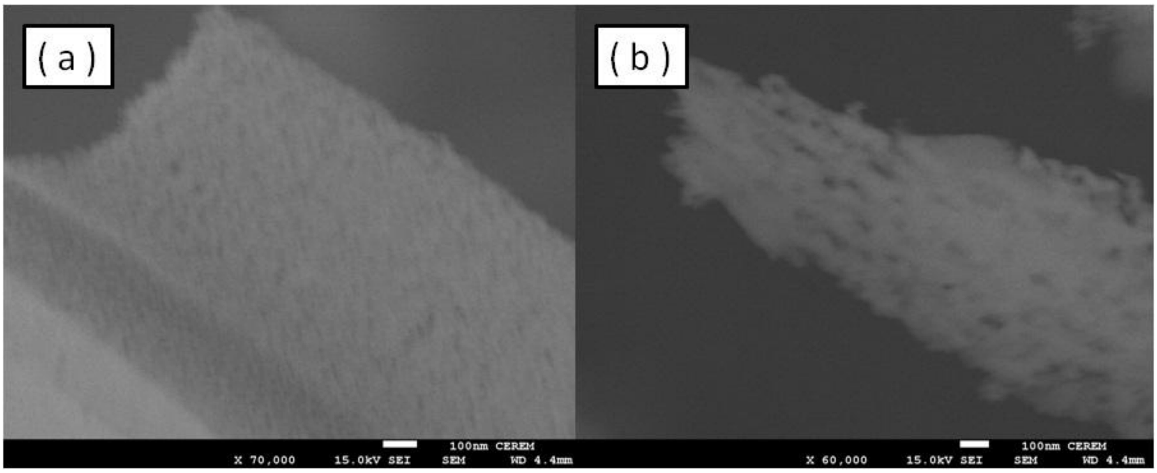

Figure 2. FESEM images electrospun fibers after calcination at 400°C for 3h in air.

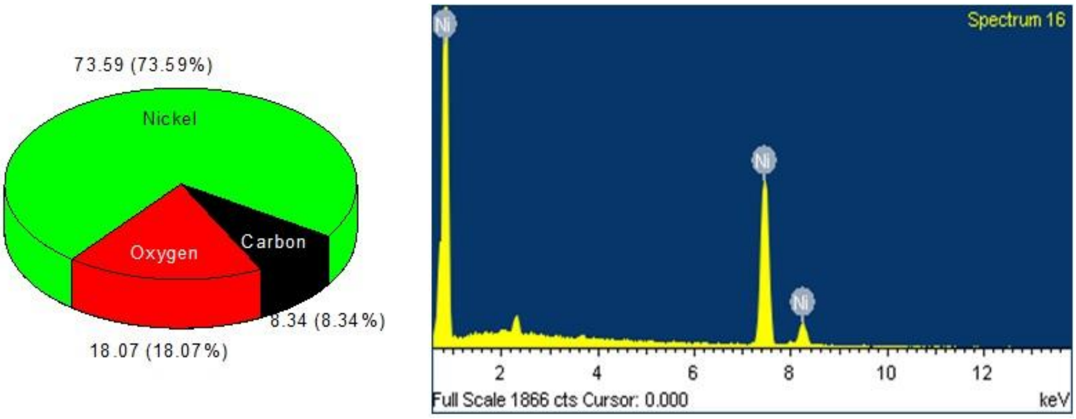

Figure 3. Elemental composition of NiO according to EDX analysis after calcination at 400°C for 3h in air.

On the other hand, the XRD data in figure 4 reveal the presence of small amount of Carbon in form of graphite, and NiO, which is consistent with the EDX results. A weak peak at about 26° was observed to indicate the presence of small amount of Graphite C 2H (ICCD 00-041-1487). The presence of graphite may be due to incomplete removal of PAN electrospun fibers template. The absence of oxygen at deep electrospun fibers layers during heat treatment may be the main reason for small amount of graphite formation.

On the other hand, the XRD patterns at 37.3°, 43.3°, and 62.8° 75.4°, and 79.4° correspond to (11 1), (2 0 0), (2 2 0), (3 1 1), and (2 2 2) cubic NiO phases respectively (ICCD 00-047-1049). Using Scherrer equation, it was possible to calculate the average grain boundary size of the prepared NiO nanostructure.

Scherrer equation: $D=\frac{K\lambda}{B\ Cos\ \theta}$ [27]

"Where D is the grain boundary size (in nm), k is the shape factor, λ is the X-ray wavelength B is the width (in radians) at half the maximum peak intensity, and θ is the Bragg angle" [27]. The calculated size for NiO calcinated at 400 °C is 20.4 nm.

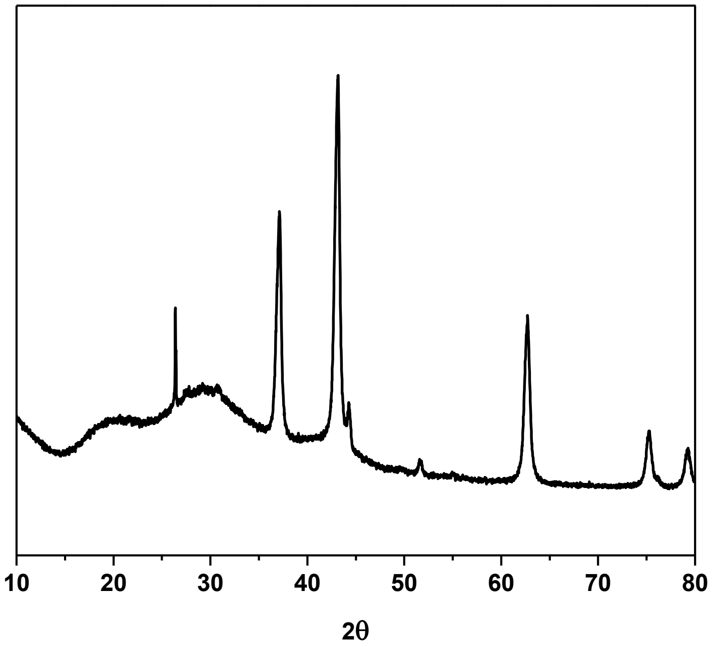

Figure 4. XRD patterns for NiO/ Nanofiber

3.2 Electrochemical Study

The electrocatalytic activity of NiO was examined in 6 M KOH and 1.0 M MeOH/6 M KOH using CV experiments within a 0.0 – 0.8 V range. The characteristic shape of the CV curves for NiO in alkaline medium is shown in Figure 4. The CV curve shows a special triangular with no sharp peaks, and a fair capacitive behavior over the 0.8 V range. Xing et al, reported the relation between calcinations temperature and capacitive behavior, where increasing the temperature of calcinations will lead to enhancing the capacitive behavior [28]. It is well know that an electrochemical active layer of $Ni(OH)_2$ will formed on the surface of NiO once electrode is immersed in alkaline medium [27].

A redox process of Ni^{2+}/Ni^{3+} according to equation 1 [27, 28]:

$Ni(OH)2 + OH^- \rightarrow NiOOH + H_2O + e^-$ (1).

The reduction peak at 0.64 V may be related to a reduction reaction of $Ni^{3+}$to Ni^{2+}, where formation of NiOOH as result of the presence of Ni^{3+} on the electrode interface to react with hydroxide ions or due to due to a reduction reaction of NiOOH to $Ni(OH)_2$ [29].

Several groups has explained the anodic and cathodic behavior, and reported the mechanism of oxidation and reduction of nickel oxy-hydroxy layer as follows [29, 30]:

$$Ni^{2+} \underset{\textbf{Reduction}}{\overset{\textbf{Oxidation}}{\rightleftarrows}} Ni^{3+} + e^- \qquad (2)$$

$$Ni^{3+} + 3OH^- \longrightarrow NiOOH + H_2O \qquad (3)$$

$$Ni(OH)_2 \underset{\textbf{Reduction}}{\overset{\textbf{Oxidation}}{\rightleftarrows}} NiOOH + H^+ + e^- \qquad (4)$$

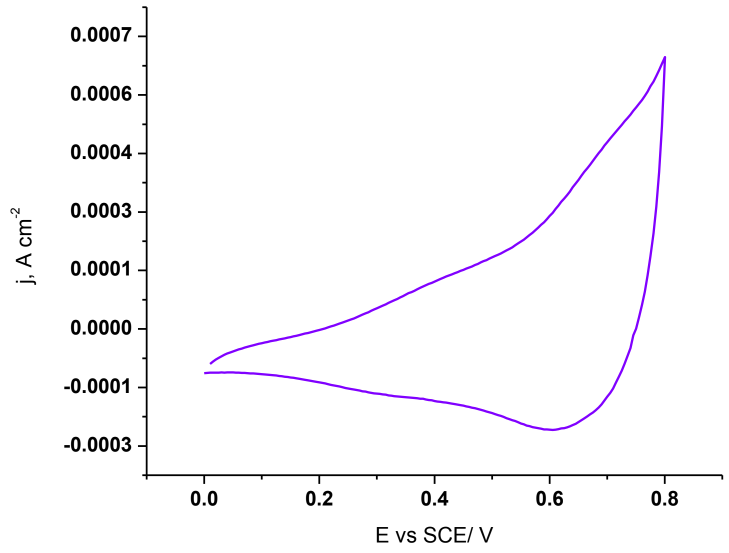

Figure 5. Cyclic voltammograms at 50 mV s^{-1} of NiO in 6 M KOH

The electrocatalytic behavior of prepared NiO was investigated . Figure 6. shows the cyclic votammograms for the oxidation of 1.0 M methanol at NiO. A significant a nodic current of methanol oxidation at onset oxidation potential of 0.47 V vs SCE is observed. This anodic peak could be related to the redox process of $Ni(OH)_2$/NiOOH conversion step [31]. It has been reported that, $Ni(OH)_2$ is presented in two different crystallographic forms; hydrous and anhydrous, α-$Ni(OH)_2$ and β-$Ni(OH)_2$ respectively.The presence of two reduction peaks at 0.45 V and 0.7 V during backward seep could be explained by the back reduction of both of β and α *forms to NiOOH* [31].

Fleischmann et al.[32] and Aziz et al.[33], have reported the main mechanism of primary alcohol oxidation, which described In the following equations:

$Ni_2(OH)+OH-\rightarrow NiOOH+H_2O+e-$ (5)
$NiOOH+RCH_2OH\rightarrow Ni\ (OH)_2+RC{\bullet}HOH$ (6)
$RC{\bullet}HOH+3OH-\rightarrow RCOOH+2H_2O+3e-$ (7)
Golikand et al. has proposed the mechanism of methanol oxidation as following [34].
$NiO + OH^- \leftrightarrow NiOOH + e^-$ (8)
$CH_3OH + NiOOH \rightarrow NiOOH(CH_3OH)_{ads}$ (9)
$NiOOH(CH_3OH)_{ads} + NiOOH \rightarrow NiO + NiOOH(CH_3OH)_{ads} + H_2O$ (10)
$NiOOH(CH_3OH)_{ads} + NiOOH \rightarrow NiO + NiOOH(COH)_{ads} + H_2O$ (11)
$NiOOH(COH)_{ads} + OH^- \rightarrow NiO + HCOO^- + H_2O$ (12)

Several products out of methanol oxidation on Ni based catalysts have been reported to be species containing formaldehyde,carbonate, and formate [27, 33, 34].

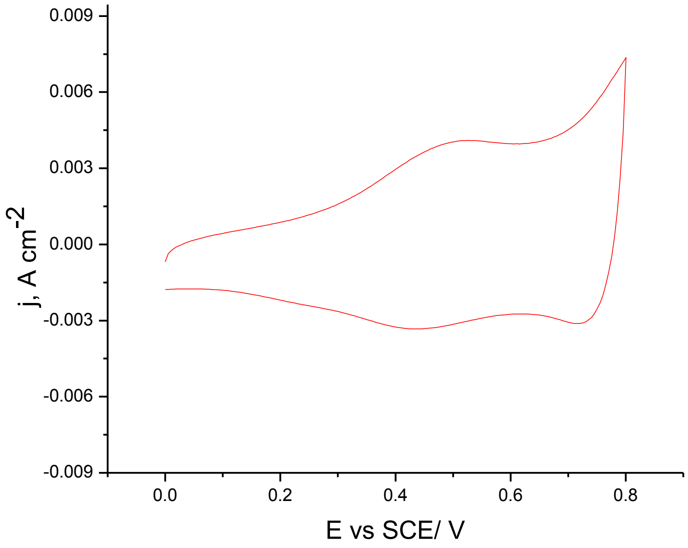

Figure 6. Cyclic voltammograms at at 50 mV s^{-1} for NiO in 1.0 M MeOH + 6 M KOH

Figure 7 shows the effect of scan rate of cyclic voltammograms of oxidation of 1.0 M methanol oxidation in 6.0 M KOH at NiO electrocatalyst. The window for methanol oxidation process at higher scan rates becomes wider in comparison with the lower scan rate, which suggests the facile electron transfer between substrate and catalytic sites.

Increasing the scan rate leads to enhancing the current peak, which could be related to diffusion or adsorption control of the process [33]. A plot of anodic peak height versus the square root of scan rate is shown in figure 8. The plot found to be linear, which suggesting that the process is diffusion rather than surface controlled [33].

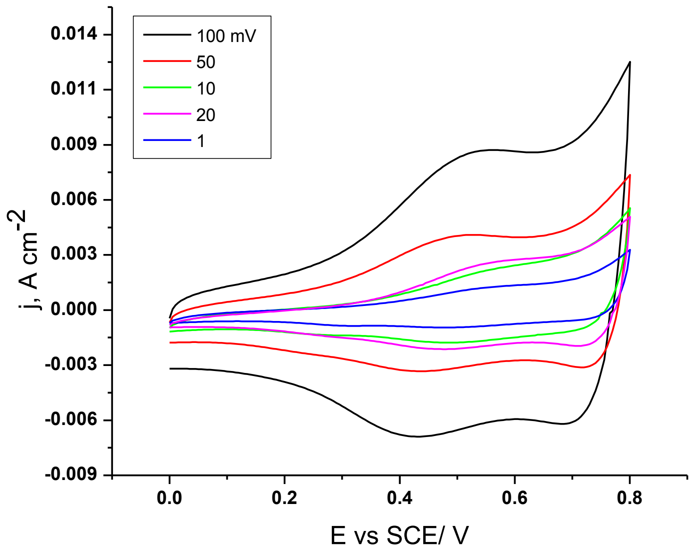

Figure 7. Cyclic voltammograms at different scanning rate for NiO in 1.0 M MeOH + 6 M KOH

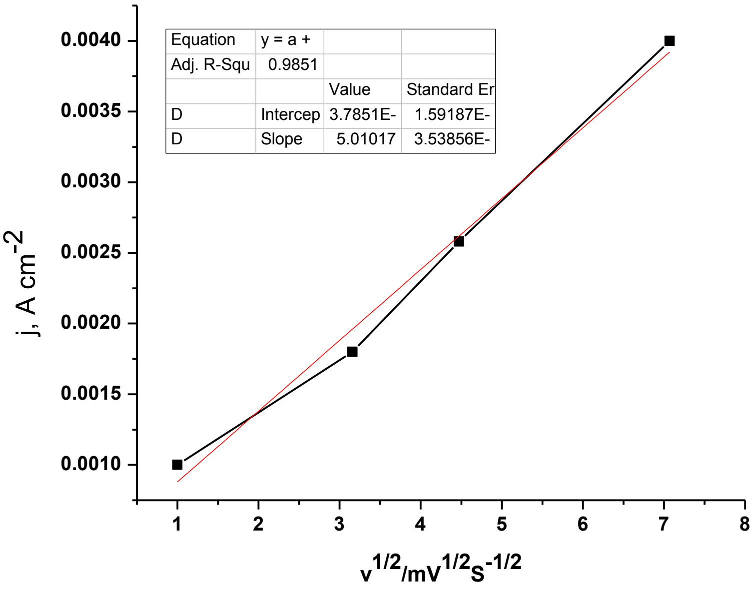

Figure 8. Variation of anodic peak height versus the square root of scan rate for oxidation of 1.0M methanol in 6.0 M KOH at NiO.

4. CONCLUSION

This work presents a facile route to synthesize NiO nanofibers using a hybrid method, which is based on a combination of electrospinning and calcination techniques.

Prepared electrospun fibers found to be a sub-micron, random, uniform fibers, and the size distribution of the produced elctrospun fibers was almost uniform and the diameter of the electrospun fibers was 145–170 nm. On the other hand, the morphology of electrospun fiber after calcinations at 400 ^oC for 3.5 h., found to have a porous structure after removal of PAN polymer template as a result of heat treatment. Prepared NiO nanostructure showed an interesting activity towards methanol oxidation. The effect of scan rate has been studied and the process has approved to be a diffusion rather than surface controlled.

ACKNOWLEDGEMENTS
The authors extend their appreciation to the Deanship of Scientific Research at King Saud University for funding the work through the research group project No RGP-VPP-227

References

1. Z.-M. Huang, Y. Z. Zhang, M. Kotaki and S. Ramakrishna. *Compos. Sci. Technol.* 63 (2003) 2223-2253.
2. Y. Wang, S. Serrano and J. J. Santiago-Aviles. *J. Mater. Sci. Lett. 21 (*2002) 1055-1057.
3. B. Ding, H. Y. Kim, S. C. Lee, C. L. Shao, D. R. Lee, S. J. Park, G. B. Kwag and K. J. Choi. *J. Polym Sci. Pol. Lett.* 40 (2002) 1261-1268.
4. A. A. E. Mahir Es-saheb, El-Sayed M. Sherif, Ahmad S. Alkaraki, El-Refaie kenawy, *Int. J. Electrochem. Sci. 7 (* 2012) 5962 - 5976.
5. J. M. Deitzel, J. D. Kleinmeyer, J. K. Hirvonen and N. C. Beck Tan. *Polymer* 42 (2001) 8163-8170.
6. I. S. Chronakis. *J. Mater. Process Tech.* 167 (2005) 283-293.
7. Y. D. W. Salalha, R. Khalfin, Y. Cohen, A. Yarin, E. Zussma. *Langmuir 19 (*2003) 7012–7020.
8. Y. Zhao, X. He, J. Li, X. Gao and J. Jia. *Sensor Actuat. B-Chem.* 165 (2012) 82-87.
9. A. E. Deniz, H. A. Vural, B. Ortac and T. Uyar. *Mater. Lett.* 65 (2011) 2941-2943.
10. D. Aussawasathien, S. Sahasithiwat, L. Menbangpung and C. Teerawattananon. *Sensor Actuat. B-Chem.* 151 (2011) 341-350.
11. S. Gautam, A. K. Dinda and N. C. Mishra. *Mat. Sci. Eng.C.* 33 (2013) 1228-1235.
12. Y.-M. Ha, T. Amna, M.-H. Kim, H.-C. Kim, M. S. Hassan and M.-S. Khil. *Colloid. Surface B.* 102 (2013) 795-802.
13. T. E. H. Fouad, Fahad N. Almajhdi, and Khalil Abdelrazek Khalil. *Int. J. Electrochem. Sci. 8* (2013) 2293 - 2304.
14. Z. Dong, S. J. Kennedy and Y. Wu. *J. Power Sources* 196 (2011) 4886-4904.
15. R. Nirmala, D. Kalpana, J. W. Jeong, H. J. Oh, J.-H. Lee, R. Navamathavan, Y. S. Lee and H. Y. Kim. *Colloid. Surface A. 384 (*2011) 605-611.
16. Y.-M. Lee and C.-H. Lai. *Solid State Electron.* 53 (2009) 1116-1125.
17. W. Zeng, B. Miao, L.-y. Lin and J.-y. Xie, *T. Nonferr. Metal. Soc.* 22 (2012) Supplement 1, s100-s104.
18. C. Ding and T. Hashida. *Int. J. Hydrogen Energ.* 36 (2011) 5567-5573.
19. Y. J. O. Asencios and E. M. Assaf. *Fuel Process. Technol.* 106 (2013) 247-252.
20. Q. X. Xia, K. S. Hui, K. N. Hui, D. H. Hwang, S. K. Lee, W. Zhou, Y. R. Cho, S. H. Kwon, Q. M. Wang and Y. G. Son. *Mater. Lett.* 69 (2012) 69-71.
21. I. T. E.O. Zayim, F.Z. Tepehan, N. Ozer. *Sol. Energy Mater. Sol. Cells* 92 (2008) 164-169.
22. G. F. Cai, C. D. Gu, J. Zhang, P. C. Liu, X. L. Wang, Y. H. You and J. P. Tu. *Electrochim. Acta,* 87 (2013) 341-347.
23. Y. Zhou, D. Gu, Y. Geng and F. Gan. *Mat. Sci. Eng. B.* 135 (2006) 125-128.
24. T. Maruyama and S. Arai. *Sol. Energy Mater. Sol. Cells* 30 (1993) 257-262.
25. B. Wang, J. L. Cheng, Y. P. Wu, D. Wang and D. N. He. Electrochem. Commun. 23 (2012) 5-8.

26. A. A. E. Abdullah M. Al-Enizi, Abdel-Rahman I. Soliman and Salem S. Al-Theyab. *Int. J. Electrochem. Sci. 7 (*2012) 12646 - 12655.
27. N. Spinner and W. E. Mustain. *Electrochim. Acta* 56 (2011) 5656-5666.
28. W. Xing, F. Li, Z.-f. Yan and G. Q. Lu. *J. Power Sources* 134 (2004) 324-330.
29. M.-S. Wu, C.-H. Yang and M.-J. Wan. *Electrochim. Acta* 54 (2008) 155-161.
30. D. Tench and L. F. Warren. *J. Electrochem. Soc.* 130 (1983) 869-872.
31. Q. Yi, J. Zhang, W. Huang and X. Liu. *Catal. Commun.* 8 (2007) 1017-1022.
32. K. K. M. Fleischmann, K. Korinek, D. Pletcher. *J. Electroanal. Chem.* 31 (1971) 39-49.
33. S. N. Azizi, S. Ghasemi and E. Chiani. *Electrochim. Acta* 88 (2013) 463-472.
34. A. N. Golikand, S. Shahrokhian, M. Asgari, M. Ghannadi Maragheh, L. Irannejad and A. Khanchi. *J. Power Sources* 144 (2005) 21-27.